Synthesis and Photoactivity of Fe_3O_4/TiO_2-Co as a Magnetically Separable Visible Light Responsive Photocatalyst

Eko Sri Kunarti*, Indriana Kartini, Akhmad Syoufian, and Karolina Martha Widyandari

Department of Chemistry, Faculty of Mathematics and Natural Sciences, Universitas Gadjah Mada, Sekip Utara, Yogyakarta 55281, Indonesia

Received July 22, 2017; Accepted January 18, 2018

ABSTRACT

Synthesis of magnetic photocatalyst, Fe_3O_4/TiO_2-Co, with characterization and photoactivity examination have been conducted. The synthesis was initiated by preparation of Fe_3O_4 particles using coprecipitation method. The Fe_3O_4 particles were then coated with TiO_2-Co at a various ratio of Fe_3O_4:TiO_2 and concentration of Co(II) dopant. The Fe_3O_4/TiO_2-Co was characterized by FTIR, XRD, TEM, SEM-EDX, VSM, and SR UV-visible methods. Photoactivity of the Fe_3O_4/TiO_2-Co was carried out using methylene blue as a target molecule in degradation reaction within a batch system. By using optimum conditions, the degradation of methylene blue solution was performed under exposure to UV, visible light and dark condition. Results showed that the Fe_3O_4/TiO_2-Co formation was confirmed by the presence of Fe_3O_4 and anatase diffraction peaks in the X-ray diffractogram. SR UV-Vis spectra indicated that the Fe_3O_4/TiO_2-Co was responsive to visible light. Band gap energy of the Fe_3O_4/TiO_2-Co with dopant concentration of 1; 5; 10 and 15% were 3.22; 3.12; 3.09 and 2.81 eV, respectively. The methylene blue solution can be well photodegraded at a pH of 10 for 210 min. The Fe_3O_4/TiO_2-Co has the highest ability to methylene blue photodegradation with dopant concentration of 10% gave degradation yield of 80.51 and 95.38% under UV and visible irradiation, respectively.

Keywords: *Fe_3O_4/TiO_2-Co; photocatalyst; methylene blue; magnetic; visible light*

ABSTRAK

Sintesis fotokatalis magnetic, Fe_3O_4/TiO_2–Co, disertai karakterisasi dan pengujian fotoaktivitasnya telah dilakukan. Penelitian diawali dengan sintesis partikel Fe_3O_4 secara kopresipitasi. Partikel Fe_3O_4 hasil sintesis kemudian dilapisi dengan TiO_2–Co pada rasio mol Fe_3O_4:TiO_2 serta konsentrasi ion Co(II) yang bervariasi. Fe_3O_4/TiO_2–Co kemudian dikarakterisasi menggunakan metode FTIR, XRD, TEM, SEM EDX, VSM dan SR UV-Visibel. Pengujian fotoaktivitas Fe_3O_4/TiO_2–Co dilakukan pada reaksi degradasi metilen biru yang dilakukan dalam sistem batch. Pengaruh konsentrasi ion Co(II) dikaji terhadap efektivitas reaksi fotokatalisis. Selanjutnya dengan menggunakan kondisi optimum, degradasi metilen biru terkatalisis Fe_3O_4/TiO_2–Co dilakukan pada paparan sinar UV, sinar tampak dan kondisi gelap. Hasil penelitian menunjukkan bahwa Fe_3O_4/TiO_2–Co dikonfirmasi keberadaannya melalui munculnya puncak Fe_3O_4 dan anatase pada difraktogram sinar-X. Spektra SR UV-Vis menunjukkan bahwa Fe_3O_4/TiO_2–Co responsif terhadap sinar tampak. Nilai energi celah pita Fe_3O_4/TiO_2–Co dengan konsentrasi dopan 1,0; 5; 10 dan 15% secara berurutan sebesar 3,22; 3,12; 3,09 dan 2,81 eV. Hasil pengujian aktivitas Fe_3O_4/TiO_2–Co menunjukkan bahwa metilen biru dapat terfotodegradasi dengan baik pada pH 10 dengan waktu reaksi selama 210 menit. Fotokatalis Fe_3O_4/TiO_2–Co memiliki kemampuan fotodegradasi paling tinggi pada konsentrasi dopan 10 % dengan nilai fotodegradasi di bawah radiasi sinar UV dan visibel masing-masing sebesar 80,51 dan 95,38%.

Kata Kunci: *Fe_3O_4/TiO_2-Co; fotokatalis; metilen biru; magnetik; sinar tampak*

INTRODUCTION

Titanium dioxide semiconductor (TiO_2) is a material often used as a photocatalyst, gas sensor, cosmetic material, corrosion protection coating and solar cell to produce hydrogen and electric energy [1-3]. TiO_2 as a photocatalyst can also be utilized in water purification, air purifiers, cancer therapies, hospital sterilization and self-cleaning equipment [4]. In recent years, TiO_2 photocatalysts are widely used in water purification as they are ideal for the degradation of organic and inorganic pollutants [3-6].

In its application as a photocatalyst, TiO_2 is active under UV light irradiation at λ <400 nm, where the maximum absorption wavelength corresponds to the band gap energy rate of 3.0–3.2 eV [7]. However, since sunlight has only about 5% of spectra in UV rays and 43% of spectra in visible light [8], the use of TiO_2 as a

* Corresponding author.
Email address : eko_kunarti@ugm.ac.id

DOI: 10.22146/ijc.26831

photocatalyst confined to UV rays is less effective when applied in the environment. The performance of TiO_2 photocatalysts could be improved by increasing optical activity by shifting the absorption of the UV to visible light. This can be conducted by providing other atoms as a dopant, increasing the sensitivity of TiO_2 with the organic or inorganic compounds that are colored (sensitizer) and electron coupling [9]. Doping technique is often done for modifying TiO_2, by providing other atoms in the form of metal and or non-metal. The doping technique results in decreasing the TiO_2 band gap energy, hence giving better performance when applied to the environment.

The transition metal, such as Cr, V, Fe, Co, W, Ce, Zr, and Cu, and non-metal like B, C, N, F, S, Cl, and Br usually was used as a dopant. The type of dopant affects the responsiveness of TiO_2 in visible light [9-10]. Doping using metal dopants is more commonly applied because of its superiority as an electron trapper that can reduce electron-hole recombination reactions.

Cobalt is one of the metals often used as a dopant to modify TiO_2 photocatalyst. Hamal and Klabunde [11] reported that the valence of the cobalt salt precursor may affect the rate of photodegradation of organic pollutants. The Co^{2+} doped TiO_2 has a faster degradation reaction time than Co^{3+} doped TiO_2 in acetaldehyde degradation under visible light irradiation with the same precursor concentration. The presence of Co dopant on TiO_2 causes the TiO_2 to have p-type conductivity. In this phenomenon, the cobalt ion acts as a scavenger or an electron capture. The doping effect of Co can decrease band gap energy (E_g) of TiO_2 shown from a shift of absorption toward longer wavelength (red shift) from diffuse reflectance UV-Visible (DR UV-Vis) spectra.

Although doping of Co^{2+} ions on TiO_2 can improve the performance of the photocatalyst, on the other hand, the photocatalyst still has problems in its use. One of the problems found in the use of TiO_2 as a photocatalyst is a difficulty of separating the TiO_2 from the liquid medium after the photocatalysis process. The TiO_2 particles in the solution tend to agglomerate when was used for a long time; resulting in decreased in the photocatalytic surface area leads to decrease in the effectiveness of photocatalysis [12]. The other problem is a trouble in recycling process due to the small size of the particles, thus requiring additional efforts to recover the TiO_2 particles from the wastewater [13]. Therefore, the addition of Fe_3O_4 material is necessary to provide the magnetic property of the photocatalyst and make the photocatalyst separable and recoverable. Photocatalysts with the magnetic properties can be synthesized by coating the surface of the magnetite core with TiO_2 nanoparticles.

Based on previous studies on the development and application of photocatalyst materials, it is interesting to combine the advantages of TiO_2 materials that can effectively be used for dyestuff degradation, dopant Co capable of shifting absorption into visible light and Fe_3O_4 which has magnetic properties, to obtain a photocatalyst that effective for dye degradation, can be performed in visible light and recoverable using an external magnetic field. In this study, we report the synthesis and photoactivity test of Fe_3O_4/TiO_2-Co as magnetically visible light and a sustainable photocatalyst.

EXPERIMENTAL SECTION

Materials

The materials used throughout these experiments were pro-analysis qualities and purchased from Merck including $FeCl_3.6H_2O$, $FeSO_4.7H_2O$, NaOH, ethanol (96%), TiO_2 Degussa, Co $(NO_3)_2.6H_2O$, and some materials with technical grade including oleic acid, methylene blue, and deionized water. All chemicals were used as received without further purification.

Instrumentation

The equipment used in this research were Fourier Transform Infrared Spectrophotometer (FTIR, Shimadzu Prestige-21), Transmission Electron Microscope (JEOL-1400 120 kV), X-Ray Diffractometer (Shimadzu XRD 6000). Scanning Electron Microscope with Energy Dispersive X-Ray (JEOL JSM-651OLA), Specular Reflectance UV-Visible Spectrometer (UV 1700 Pharmaspec UV-Vis Spectrophotometer Specular), and vibrating sample magnetometer (Oxford VSM 1.2H).

Procedure

Synthesis of Fe_3O_4 particles

An amount of 3.89 g of $FeCl_3.6H_2O$ and 2.015 g $FeSO_4.7H_2O$ were dissolved in 30 mL of deionized water, then the solution was added to 60 mL of 3 M NaOH solution dropwise while it was ultrasonicated. The precipitation of Fe_3O_4 formed was added with 1 g of oleic acid while ultrasonicated for 1 h. The precipitate formed was separated by an external magnetic bar and washed with distilled water until neutral, then it was dried in the oven at 90 °C for 2 h.

Synthesis of Fe_3O_4/TiO_2

The Fe_3O_4 particles from the previous stage were added with TiO_2 Degussa, suspended in 30 mL of ethanol 96% and sonicated for 30 min for forming a

suspension. Fe_3O_4/TiO_2 particles were prepared with a variation of Fe_3O_4 to TiO_2 mole ratio of 1:3; 1:10 and 1:15. The particles were then deposited and separated from the solution by an external magnetic bar. Subsequently, the sample was dried in an oven at 90 °C for 3 h and was calcined at 500 °C for 4 h.

Synthesis of Fe_3O_4/TiO_2-Co

Two grams of TiO_2 Degussa was suspended in 25 mL of ethanol 96% while ultrasonicated. The suspension was then added dropwise with a solution of $Co(NO_3)_2.6H_2O$ that was dissolved in 10 mL of distilled water with a variable concentration of 1, 5, 10, and 15% (w/w) while sonicating for 30 min. The mixture was added with Fe_3O_4 particles and suspended in 96% ethanol from the previous stage with the best Fe_3O_4:TiO_2 ratio of 1:10 while being sonicated for 30 minutes. The particles were then deposited and separated from the solution by an external magnetic bar. The sample was subsequently dried in an oven at 90 °C for 3 h, then calcined at 500 °C for 4 h.

Photoactivity of Fe_3O_4/TiO_2-Co

About 10 mg photocatalysts of TiO_2, Fe_3O_4/TiO_2 with a ratio of (1:10) and Fe_3O_4/TiO_2-Co in all variations dopant concentration (1, 5, 10, and 15%) were each added to 10 mL of methylene blue solution 5 mg/L at a pH of 10 [14]. Photodegradation was performed under stirring for 210 min with a variety conditions: dark, under UV illumination, and visible irradiation. After photodegradation process, the photocatalyst was then separated by centrifugation for TiO_2 and using an external magnetic field for Fe_3O_4/TiO_2 and Fe_3O_4/TiO_2-Co. The filtrate was then analyzed by UV-visible spectrophotometry at the optimum wavelength of methylene blue solution (660 nm).

RESULT AND DISCUSSION

Effect of Fe_3O_4 to TiO_2 Molar Ratio

Titania was coated on the Fe_3O_4 surface by dispersion method in ethanol followed by thermal treatment. Ethanol is used as a medium for TiO_2 to cover the Fe_3O_4 surface. The TiO_2 is varied with a molar ratio of 3:1, 10:1, and 15:1 to Fe_3O_4. The molar variation of TiO_2 was intended to obtain high photocatalyst activity while the presence of Fe_3O_4 to provide magnetic properties for facilitating the photocatalyst retrieval process. In this study, the best molar ratio of Fe_3O_4 to TiO_2 was then chosen as the material to be doped with Co(II).

Fig. 1 displays infrared spectra of Fe_3O_4 and Fe_3O_4/TiO_2 with a various molar ratio of Fe_3O_4 to TiO_2. It can be seen that Fe_3O_4/TiO_2 spectra have a higher absorption intensity than Fe_3O_4 at the wave numbers of 2337 and 500–700 cm^{-1}, respectively, due to the contribution of stretching and bending Ti-O of TiO_2 on Fe_3O_4 surface. Meanwhile, the intensity of Fe_3O_4/TiO_2 at wave numbers of 2337 and 500–700 cm^{-1} increases with increasing mole of TiO_2.

X-ray diffraction pattern in Fig. 2 shows that some peaks appear at 2θ: 25, 38, 48, 53, 62 and 75° for the Fe_3O_4/TiO_2 diffractogram for all molar ratios, where the peaks are not owned by Fe_3O_4 before coating of TiO_2. These peaks are typical peaks of TiO_2 anatase, corresponding to the Miller index in JCPDS number 89-4203 with the (hkl) values being: (101), (112), (200),

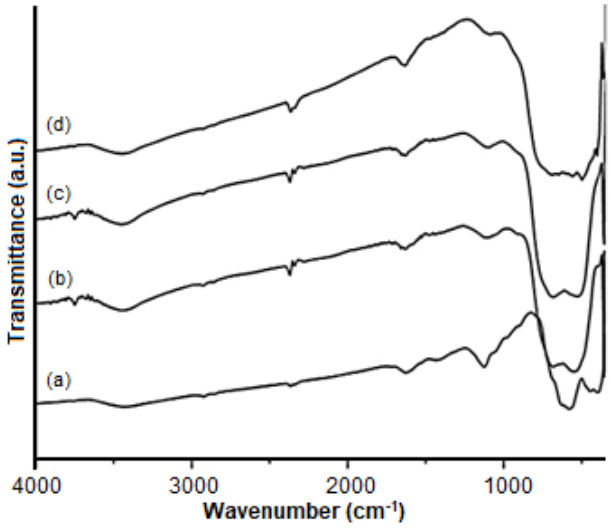

Fig 1. Infrared spectra of Fe_3O_4 (a), Fe_3O_4/TiO_2 with molar ratio of 1:3 (b) 1:10 (c) 1:15 (d)

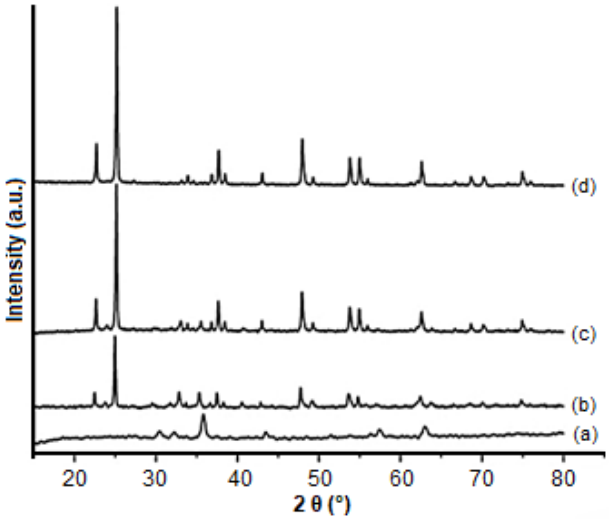

Fig 2. The X-ray diffraction pattern of Fe_3O_4 (a) Fe_3O_4/TiO_2 with molar ratio of 1:3 (b) 1:10 (c) 1:15 (d)

(105), (213) and (215), respectively, indicating the anatase phase of titania.

It can also be seen in Fig. 2 that the intensity of the anatase peaks increases with the increasing concentration of the TiO_2. This means that the presence of anatase phase of TiO_2 in Fe_3O_4/TiO_2 is also increased. On the other hand, in the Fe_3O_4/TiO_2 diffractogram, there is a decrease in the intensity of the characteristic peaks of Fe_3O_4 as more TiO_2 was added. This implies that TiO_2 increasingly coats the Fe_3O_4 surface.

In this study, the optimum mole ratio of Fe_3O_4 to TiO_2 was determined by a quantitative test of materials that can be drawn by an external magnetic field with the results are displayed in Table 1. It is shown in the table that percentage of magnetic attraction of Fe_3O_4/TiO_2 material with a molar ratio of 1:15 declines. This is because of the higher the molar ratios, the more moles of TiO_2 coat the Fe_3O_4 surface, so the attraction to the external magnet decreases. Data in Table 1 corresponds to the X-ray diffraction pattern indicating that there is a decrease in the intensity of the Fe_3O_4 peaks along with the increasing concentration of TiO_2. So Fe_3O_4/TiO_2 material with the molar ratio of 1:10 was taken as the molar ratio of the TiO_2, which then added to the Fe_3O_4.

Table 1. The percentage of attraction of material to external magnetic

Material	% magnetic attraction
Fe_3O_4/TiO_2 (1:3)	100
Fe_3O_4/TiO_2 (1:10)	100
Fe_3O_4/TiO_2 (1:15)	84.21

Table 2. The 2θ of the photocatalyst samples

Photocatalyst	2θ (°)	d (Å)
Fe_3O_4/TiO_2	25.1333	3.5404
Fe_3O_4/TiO_2–Co (1%)	25.4980	3.4906
Fe_3O_4/TiO_2–Co (5%)	25.6775	3.4666
Fe_3O_4/TiO_2–Co (10%)	25.4484	3.4973
Fe_3O_4/TiO_2–Co (15%)	25.0177	3.5565

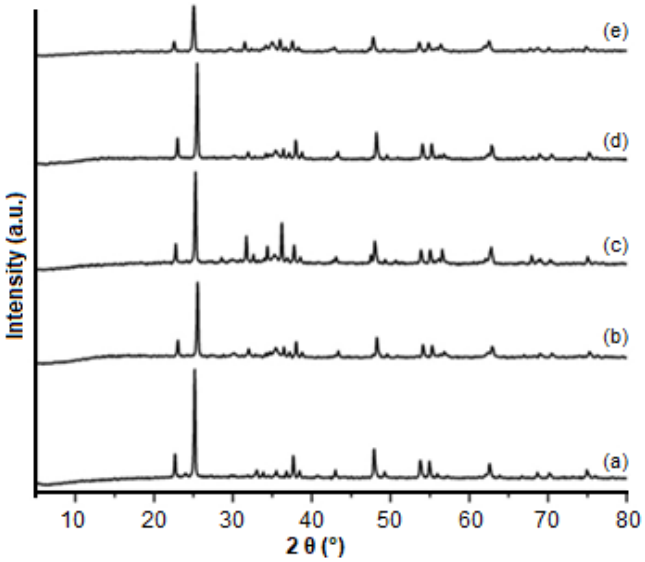

Fig 3. X-ray diffraction pattern of Fe_3O_4/TiO_2 (a) Fe_3O_4/TiO_2–Co 1% (b) 5% (c) 10% (d) 15% (e)

Effect of Dopant Concentration

Fig. 3 presents the X-ray diffraction pattern of Fe_3O_4/TiO_2 and Fe_3O_4/TiO_2-Co with a variety of dopant concentrations of Co(II). There are some characteristic peaks of magnetite and anatase of Fe_3O_4/TiO_2 and Fe_3O_4/TiO_2-Co samples. The peaks of Fe_3O_4 characteristics are shown at the 2θ of 29.81; 35.12; 42.89; 56.62 and 62.30°, while anatase is revealed in 25, 38, 48, 53, 62, and 75°. There is no characteristic peak of Co(II) dopant appear at the Fe_3O_4/TiO_2-Co for all variations of the dopant concentration, which may be attributed to the relatively lower Co(II) content and uniform dispersion on TiO_2 as also reported in other studies [15]. There were possibilities that the dopant was in the crystal lattice by substituting Ti^{4+} position or on the surface of the crystal lattice of TiO_2.

Diffractogram in Fig. 3 shows also that at the 2θ around 25°, the Fe_3O_4/TiO_2–Co for all variations of dopant concentrations have a lower intensity than that of Fe_3O_4/TiO_2. The decrease in the intensity indicates that dopants successfully substitute Ti^{4+}. On the other hand, the Fe_3O_4/TiO_2-Co peak intensity tends to increase with increasing concentration of dopant (up to 10%), confirming that the dopant does not damage the crystal structure. This also implies that the Co(II) dopants were attached to the crystal structure of TiO_2. However, for the Fe_3O_4/TiO_2-Co with the dopant concentration of 15%, a decline in intensity was observed. This is possible because of some Co^{2+} substitute Ti^{4+} within the structure of TiO_2. It is also seen in Fig. 3 that there is shifted off the 2θ around 25° of the Fe_3O_4/TiO_2-Co toward the greater 2θ. This indicates that modification with Co(II) dopant affected the distance between planes. It suggests that the dopant was at an interstitial position within the crystal lattice of TiO_2, resulting in the smaller distance between planes in the crystal lattice of Fe_3O_4/TiO_2-Co than that of un-doped Fe_3O_4/TiO_2.

Table 2 shows that the 2θ approximately 25° of Fe_3O_4/TiO_2-Co (15%) is shifted toward smaller 2θ than that of Fe_3O_4/TiO_2. This denotes that there is a substitution of Co^{2+} with Ti^{4+} causing the distance between the planes of Fe_3O_4/TiO_2-Co (15%) greater than that of Fe_3O_4/TiO_2. It may be attributed to the radius of Co^{2+}. The Co^{2+} radius is larger than that of Ti^{4+} in the crystal lattice of TiO_2 that leads to the extension of the lattice parameter values in it hence larger distance between the planes. Table 3 depicts average crystallite size of Fe_3O_4/TiO_2 and Fe_3O_4/TiO_2–Co. It is

shown in Table 3 that the synthesized materials have small crystallite size. This suggests that the Co(II) dopant inhibits the growth of Fe_3O_4/TiO_2-Co particles. This result is in agreement with the report by Hamadanian et al. [16] in the synthesis of TiO_2-Co.

Magnetic Property of Fe_3O_4/TiO_2-Co

Magnetic property of the synthesized Fe_3O_4/TiO_2-Co material was quantitatively tested by measuring magnetism using the VSM. The VSM result shown in Fig. 4 designates that both Fe_3O_4/TiO_2 and Fe_3O_4/TiO_2-Co have good superparamagnetic properties as in the common Fe_3O_4 particles with the magnetism value of Fe_3O_4/TiO_2-Co is smaller compared to that of Fe_3O_4/TiO_2 without Co. The decline in magnetic properties of the material due to the thick layer of TiO_2-Co that coats the Fe_3O_4 nanoparticles.

Morphology of Fe_3O_4/TiO_2-Co

Morphology of Fe_3O_4/TiO_2-Co was analyzed by TEM as displayed in Fig. 5. It is clearly shown that Fe_3O_4/TiO_2-Co material is spherical particles with no agglomeration. Fig. 5 also shows that gray layer of TiO_2 particles coats the dark color of Fe_3O_4 with core-shell structure. Since Co is substituted into the TiO_2 structure, its presence becomes part of the TiO_2 quilt and does not exhibit certain characteristics color. The darker color portion is due to a combination of some crystalline materials of Fe_3O_4 and TiO_2. Overall, TEM image shows the Fe_3O_4 with dark spherical shades and gray blankets referring to TiO_2. Based on Fig. 5, the Fe_3O_4 nanoparticles have an average size of 13 nm, while Fe_3O_4/TiO_2-Co (10%) having an average size of 20 nm. The result proves that in this study, Fe_3O_4/TiO_2-Co material has been successfully synthesized.

Based on the SEM-EDX spectrum in Fig. 6, the Fe_3O_4 /TiO_2-Co consists of O (44.05%), Na (4.34%), S (0.93%), Cl (0.58%), Ti (5.98%), Fe (41.79%) and Co (2.33%) elements on the surface of the material. The presence of Na, S, and Cl possibility come from the impurities in the Fe_3O_4 material. The Na element may be derived from NaOH solution while S and Cl possibly come from $FeSO_4.7H_2O$ and $FeCl_3.6H_2O$ salts used in the synthesis of Fe_3O_4. The SEM-EDX data confirms that the as-synthesized material is Fe_3O_4/TiO_2-Co.

Electronic Property of Fe_3O_4/TiO_2-Co

Characterization using SR UV-Vis method was aimed to determine the absorption edge wavelength and band gap energy (E_g) of the Fe_3O_4/TiO_2-Co. Both the

Table 3. Average crystallite size of Fe_3O_4/TiO_2 and Fe_3O_4/TiO_2–Co

Materials	d (nm)
Fe_3O_4	16.67
Fe_3O_4/TiO_2 (1:3)	43.46
Fe_3O_4/TiO_2 (1:10)	43.41
Fe_3O_4/TiO_2 (1:15)	44.07
Fe_3O_4/TiO_2–Co (1%) (1:10)	38.62
Fe_3O_4/TiO_2–Co (2.5%) (1:10)	40.30
Fe_3O_4/TiO_2–Co (10%) (1:10)	41.64
Fe_3O_4/TiO_2–Co (15%) (1:10)	29.61

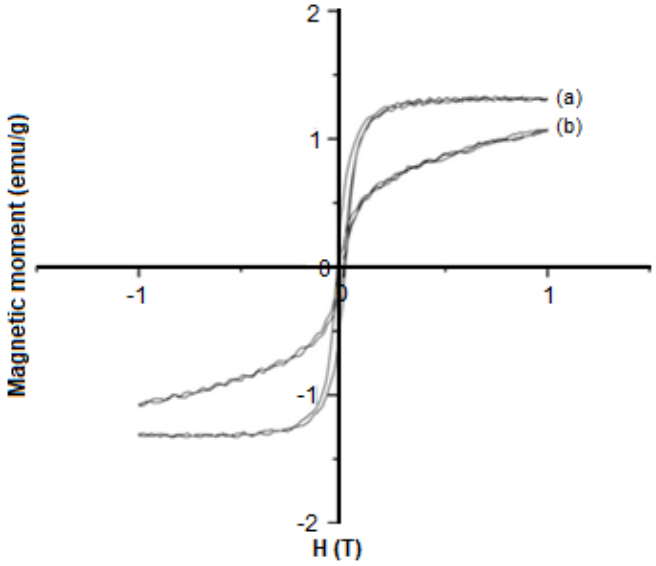

Fig 4. Magnetic moment curve of Fe_3O_4/TiO_2 (a) and Fe_3O_4/TiO_2-Co (b)

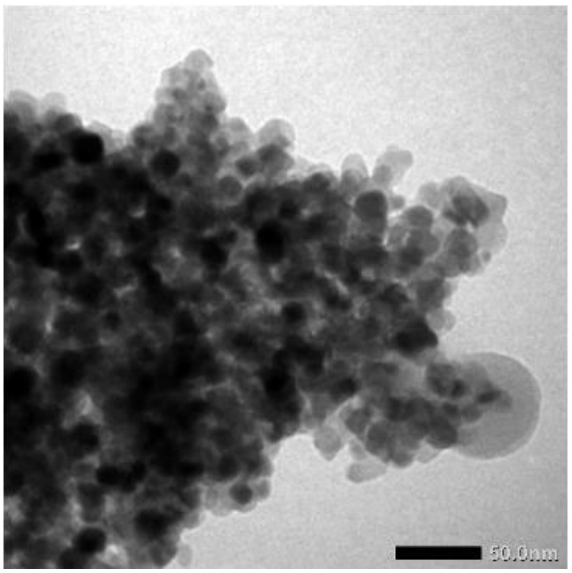

Fig 5. TEM image of Fe_3O_4/TiO_2-Co

absorption edge and the E_g are correlated with the responsiveness of Fe_3O_4/TiO_2-Co to light energy. Fig. 7 reveals that there is a shift of absorption wavelength toward the visible light with increasing concentration of Co(II). Fig. 7 also shows that the Fe_3O_4/TiO_2-Co for all variations concentration of dopant give new absorption with low intensity at a wavelength of 439, 424, 436, and 457 nm for the dopant concentration of 1, 5, 10 and 15%, respectively.

Table 4 demonstrates that Fe_3O_4/TiO_2–Co samples have absorption edge wavelength greater than that of TiO_2. The Fe_3O_4/TiO_2–Co wavelength increases with the increasing concentration of Co^{2+} dopants. This suggests a shift of edge from the UV to the visible light region. The absorption edge wavelength is inversely proportional to the value of E_g so the greater the absorption edge wavelength value, the smaller the E_g value.

Based on the calculation, it can be known that TiO_2 anatase has the value of E_g 3.24 eV. This is consistent with the result of Mital and Manoj [17] who reported that anatase phase of free TiO_2 has an E_g value of 3.20 eV, where the bandgap energy corresponds to the energy in the UV light wavelength region. The results showed that Fe_3O_4/TiO_2–Co in all concentrations of Co^{2+} dopant have a smaller E_g value than un-doped TiO_2. The greater the concentration of Co^{2+} dopant added, the more likely that Co^{2+} ions were trapped both interstitial and substitutional within the TiO_2 crystal lattice. The addition of Co^{2+} ion can decrease the E_g value of TiO_2 and make the Fe_3O_4/TiO_2–Co is responsive to visible light.

Several characterizations that have been done suggest that the Fe_3O_4/TiO_2–Co have been successfully synthesized. The Fe_3O_4/TiO_2–Co is responsive to visible rays as proven by the occurrence of redshifts of absorption edge wavelength to the visible light region with smaller E_g values than the un-doped anatase TiO_2. The Fe_3O_4/TiO_2–Co has a magnetic character of Fe_3O_4 nanoparticles, this allows the Fe_3O_4/TiO_2–Co to be easily separated and recovered from the liquid medium by using an external magnetic field.

Photoactivity of the Fe_3O_4/TiO_2-Co

The photocatalytic activity of Fe_3O_4/TiO_2–Co was examined to degrade the 5 mg/L methylene blue solution. The methylene blue photodegradation was performed using 10 mg photocatalyst at a pH of 10 under UV light, visible light exposure and dark condition no irradiation for 210 min. The light serves as the energy source for Fe_3O_4/TiO_2–Co to perform photocatalysis reactions. The energy in the form of photons ($h\nu$) will be absorbed by Fe_3O_4/TiO_2–Co, thereby producing •OH radical, which plays a role in the methylene blue degradation reaction. The reaction involved the capture and release of electrons caused by photon energy. Photodegradation is carried out in reactors equipped with stirring and radiation sources. Stirring serves to accelerate the occurrence of contact between the photocatalyst materials with methylene blue. The methylene blue solution after the degradation process was analyzed using a UV-Vis spectrophotometer at its maximum absorption wavelength of 660 nm.

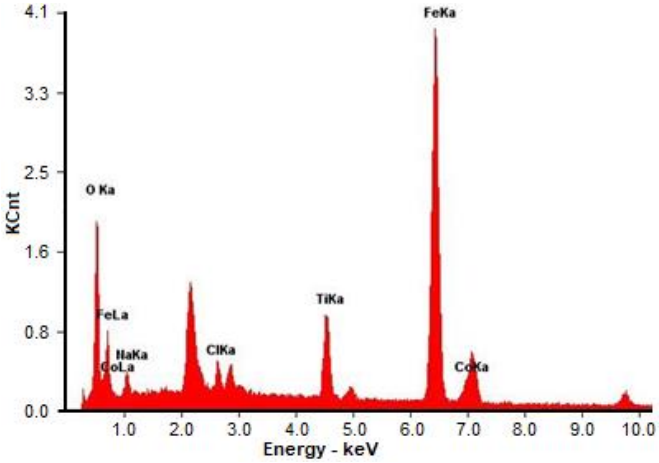

Fig 6. SEM-EDX spectrum of Fe_3O_4/TiO_2-Co

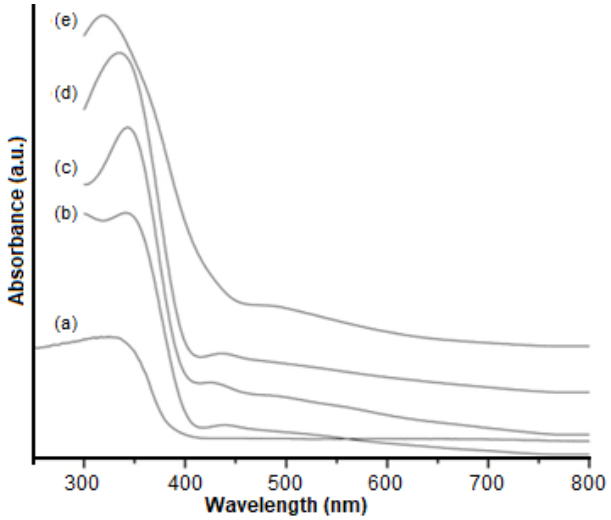

Fig 7. SR UV-Visible spectra of TiO_2 (a), Fe_3O_4/TiO_2–Co with the dopant concentration of 1% (b); 5% (c); 10% (d) and 15% (e)

Table 4. Absorption edge wavelength and bandgap energy of TiO_2 and Fe_3O_4/TiO_2–Co

Material	λ edge (nm)	E_g (eV)
TiO_2	382.69	3.24
Fe_3O_4/TiO_2–Co (1%)	385.47	3.22
Fe_3O_4/TiO_2–Co (5%)	397.59	3.12
Fe_3O_4/TiO_2–Co (10%)	401.35	3.09
Fe_3O_4/TiO_2–Co (15%)	438.08	2.81

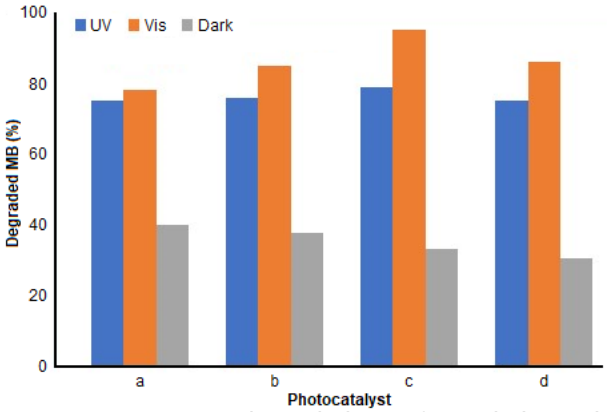

Fig 8. Percentage degradation of methylene blue catalyzed by Fe_3O_4/TiO_2–Co 1% (a), 5% (b), 10% (c) and 15% (d)

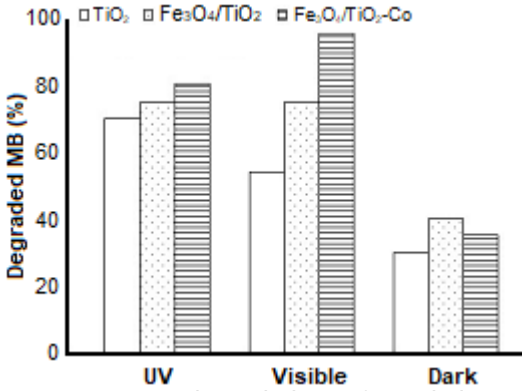

Fig 9. Percentage degradation of methylene blue-catalyzed by TiO_2, Fe_3O_4/TiO_2, and Fe_3O_4/TiO_2–Co (10%)

The photodegradation process requires a source of light energy for the reaction to occur. According to Fig. 8, it can be recognized that Fe_3O_4/TiO_2–Co photocatalysts can degrade methylene blue even without irradiation. This is due to the occurrence of adsorption process before degradation in photocatalytic reaction, as reported by Belessi et al. [18]; TiO_2 in dark spaces can adsorb the reactive red dyes characterized by the reduced concentration of the dye. The presence of Fe_3O_4 can also act as a good adsorbent [19]. Fig. 8 revealed that in the non-irradiated process there is a decrease in activity as the concentration of dopant increases. This probably because more Co^{2+} dopants substitute Ti^{4+}, so the function of TiO_2 as the adsorbent is reduced.

The photocatalytic activity of Fe_3O_4/TiO_2–Co under UV light irradiation decreased with increasing concentration of Co^{2+}. This is mainly caused by incompatibility of band gap energy with the wavelength of the UV light. This is in contrasts with photodegradation activity under visible light illumination, where photocatalytic activity increases with increasing concentration of Co^{2+} dopant. The more concentration of Co^{2+} increases the responsiveness to visible light, resulting in a greater percentage of degradation. In addition, it can also be seen that percentage degradation in visible light irradiation is greater than those of UV irradiation. This suggests that Fe_3O_4/TiO_2-Co photocatalysts are more responsive to visible light than UV light.

Fig. 9 shows that Fe_3O_4/TiO_2-Co with the concentration of Co(II) 10% gave the highest photocatalytic activity compared to pure TiO_2 and un-doped Fe_3O_4/TiO_2 at a pH of 10 for 210 min of degradation time. Fig. 9 indicates that Fe_3O_4/TiO_2 (1:10) and Fe_3O_4/TiO_2-Co (10%) can degrade more methylene blue than TiO_2 due to the contribution of Fe_3O_4, which acts as an adsorbent. In addition, according to Fig. 9, it can also be perceived that in the visible irradiation processes, the Fe_3O_4/TiO_2 photocatalyst gives greater % degradation than pure TiO_2 owing to the contribution of Fe_3O_4 material that can adsorb the same methylene blue as in UV irradiation. The Fe_3O_4/TiO_2-Co photocatalyst degrades more methylene blue than that of the Fe_3O_4/TiO_2 proving that the presence of Co^{2+} dopants can improve the performance of photocatalysts in the visible light region. Non-irradiated degradation reactions may also decrease the concentration of methylene blue, but the resulting % degradation is less than that of UV and visible irradiation as there was only the adsorption process occurred. Fig. 9 revealed that % degradation of Fe_3O_4/TiO_2-Co (10%) under visible illumination is larger than that of unmodified TiO_2. This indicates that the Fe_3O_4/TiO_2-Co photocatalyst is more responsive to visible light than TiO_2. The Fe_3O_4/TiO_2-Co will be more effectively used as a photocatalyst than unmodified TiO_2.

CONCLUSION

Fe_3O_4/TiO_2-Co particles were synthesized through coprecipitation method and dispersion with ethanol followed by thermal treatment. The addition of Co(II) decreases the band gap energy of TiO_2 from 3.24 to 2.81 eV. The Fe_3O_4/TiO_2-Co particles are responsive to visible light. The Fe_3O_4/TiO_2-Co can be used as photocatalyst for methylene blue degradation under UV and visible light exposure and have adsorption ability in dark conditions. The Fe_3O_4/TiO_2-Co with the mass of 10 mg is capable of degrading 5 mg/L of methylene blue solution at a pH of 10 under UV and visible light irradiation for 210 min with the degradation yield of 80.51 and 95.38%, respectively. The Fe_3O_4/TiO_2-Co photocatalyst has good magnetic properties and can be

easily recovered from the liquid medium by using an external magnetic field.

ACKNOWLEDGEMENT

The authors acknowledge to The Directorate General of Higher Education, Ministry of Research Technology and the Higher Education Republic of Indonesia, and Universitas Gadjah Mada for the financial support.

REFERENCES

[1] Hoffmann, M.R., Martin, S.T., Choi, W., and Bahnemann, D.W., 1995, Environmental applications of semiconductor photocatalysis, *Chem. Rev*., 95 (1), 69–96.

[2] Yin, S., Liu, B., Zhang, P., Morikawa, T., Yamanaka, K., and Sato, T., 2008, Photocatalytic oxidation of under visible led light irradiation over nitrogen-doped titania particles with iron or platinum loading, *J. Phys. Chem. C*, 112 (32), 12425–12431.

[3] Qiu, R., Zhang, D., Diao, Z., Huang, X., He, C., Morel, J.L., and Xiong, Y., 2012, Visible light induced photocatalytic reduction of Cr(VI) over polymer-sensitized TiO_2 and its synergism with phenol oxidation, *Water Res.*, 46 (7), 2299–2306.

[4] Shen, Y., Xiong, T., Du, H., Jin, H., Shang, J., and Yang, K., 2009, Phosphorous, nitrogen, and molybdenum ternary co-doped TiO_2: Preparation and photocatalytic activities under visible light, *J. Sol-Gel Sci. Technol.*, 50 (1), 98–102.

[5] Xu, C., Rangaiah, G.P., and Zhao, X.S., 2014, Photocatalytic degradation of methylene blue by titanium dioxide: experimental and modeling study, *Ind. Eng. Chem. Res*., 53 (38), 14641–14649.

[6] Kunarti, E.S., Syoufian, A., Budi, I.S., and Pradipta, A.R., 2016, Preparation and properties of $Fe_3O_4/SiO_2/TiO_2$ core-shell nanocomposite as recoverable photocatalyst, *Asian J. Chem.*, 28 (6), 1343–1346.

[7] Daghrir, R., Drogui, P., and Robert, D., 2013, Modified TiO_2 for environmental photocatalytic applications: A review, *Ind. Eng. Chem. Res*., 52 (10), 3581–3599.

[8] Kumar, S.G., and Devi, L.G., 2011, Review on modified TiO_2 photocatalysis under UV/visible light: Selected result and related mechanisms on interfacial charge carrier transfer dynamics, *J. Phys. Chem. A*, 115 (46), 13211–13241.

[9] Chen, X., and Mao, S.S., 2007, Titanium dioxide nanomaterials: synthesis, properties, modifications, and applications, *Chem. Rev*., 107 (7), 2891–2959.

[10] Choi, J., Park, H., and Hoffmann, M.R., 2010, Effects of single metal-ion doping on the visible-light photoreactivity of TiO_2, *J. Phys. Chem. C*, 114 (2), 783–792.

[11] Hamal, D.B., and Klabunde, K.J., 2011, Valence state and catalytic role of cobalt ions in cobalt TiO_2 nanoparticle photocatalysts for acetaldehyde degradation under visible light, *J. Phys. Chem. C*, 115 (35), 17359–17367.

[12] Pozzo, R.L., Baltanás, M.A., and Cassano, A.E., 2010, Supported titanium dioxide as photocatalyst in water decontamination: State of the art, *Catal. Today*, 39 (3), 219–231.

[13] Liu, H., He, Y., and Liang, X., 2013, Magnetic photocatalysts containing TiO_2 nanocrystals: Morphology effect on photocatalytic activity, *J. Mater. Res*., 29 (1), 98–106.

[14] Widyandari, K.M., 2016, Sintesis Nanokomposit Fe_3O_4/TiO_2-Co dan Uji Aktivitasnya sebagai Fotokatalis, *Undergraduate Thesis*, Universitas Gadjah Mada, Yogyakarta.

[15] Chatti, R., Rayalu, S.S., Dubey, N., Labhsetwar, N., and Devotta, S., 2007, Solar-based photoreduction of methyl orange using zeolite supported photocatalytic materials, *Sol. Energy Mater. Sol. Cells*, 91 (2-3), 180–190.

[16] Hamadanian, M., Reisi-Vanani, A., and Majedi, A., 2010, Sol-gel preparation and characterization of Co/TiO_2 nanoparticles: applications to the degradation of methyl orange, *J. Iran. Chem. Soc*., 7 (Suppl. 2), S52–S58.

[17] Mital, G.S., and Manoj, T., 2011, A review of TiO_2 nanoparticles, *Chin. Sci. Bull.*, 56 (16), 1639–1657.

[18] Belessi, V., Romanos, G., Boukos, N., Lambropoulou, D., and Trapalis, C., 2009, Removal of reactive red 195 from aqueous solutions by adsorption on the surface of TiO_2 nanoparticles, *J. Hazard. Mater.*, 170 (2-3), 836–844.

[19] Abkenar, S.D., 2016, Application of magnetic-modified Fe_3O_4 nanoparticles for removal of crystal violet from aqueous solution: Kinetic, equilibrium and thermodynamic studies, *J. Appl. Chem. Res.*, 10 (1), 65–74.